Conf-9310102--38

BNL-49639

ON THE LIQUEFACTION FAILURE OF AN EARTH DAM *

Nikolaos Simos and Morris Reich
Department of Advanced Technology
Brookhaven National Laboratory
Upton, NY 11973

with
Carl J. Costantino
Department of Civil Engineering, City College of New York
Convent Avenue at 137th Str., New York, NY 11028

RECEIVED
DEC 14 1993
OSTI

ABSTRACT

In an effort to better assess the potential for sliding and liquefaction failure of earthen dams when subjected to earthquake loadings, a dynamic finite element approach focusing on these two failure mechanisms as well as on the vital role of the pore water pressure was undertaken.

The constitutive response of the granular soil skeleton and its coupling with the fluid phase is formulated based on the Biot dynamic equations of motion. The constitutive model for the soil material was assumed to be linear with nonlinear terms included in the hysteretic damping terms. Despite the linear character of this theoretical model, one can still draw important conclusions regarding the stability and the liquefaction resistance of the cross-section.

As an example, a hypothetical earth dam constructed over a saturated soil layer was considered. The steady state conditions of *in-situ* stress and pore pressure distributions in both the embankment and the foundation are evaluated and implemented in the stability and liquefaction criteria in conjunction with the dynamic analysis. The latter is carried out in the frequency domain and it reflects the response of the dam-foundation system to a seismic excitation. The computational aspect of the study is performed with finite element analysis. A transmitting boundary formulation for the two phase material was used to treat the infinite space problem.

It is anticipated that the intensity of the earthquake input and certain soil properties have a profound effect on the failure susceptibility of the dam section. To address the uncertainties regarding the true values of such parameters, the analysis considered them parametrically.

* This work was performed under the auspices of the U.S. Department of Energy.

INTRODUCTION

During an earthquake event of considerable duration and intensity an earthen dam can experience partial or total failure that stems from either loss of soil strength due to liquefaction or reduction of the inherent resistance to sliding along a potential failure surface. In order to evaluate the response of a typical dam section and from it assess the failure potential, the model shown in Figure 1 was chosen as a case study. Specifically, the tailings dam consisting of a core and upstream and downstream shells is constructed atop a soil layer which in turn lies over the bedrock. The upstream pool of water induces seepage flow through the embankment and the foundation layer. During a seismic event, the pore pressure increases while the effective stress in the soil decreases leading to considerable loss of strength (shear strength is controlled by effective stress).

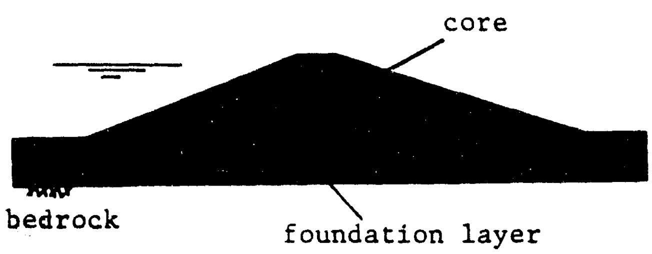

Figure 1. Model of Dam Cross Section.

It is apparent that any analysis of earthen dams should address the seismic stability concerns by considering all the mechanisms that seem to play a role, namely

- Seepage forces generated by the steady state flow of water through the dam and its foundation.
- Soil properties within the embankment that dictate both the amount of seepage as well as the inherent strength of the structure.
- Driving forces along potential failure surfaces that determine the level of safety against slope sliding and failure for the entirety of the seismic event.
- Selection of the appropriate earthquake input which best represents the seismic hazard t the particular site.
- Evaluation of the soil profile in the embankment and the foundation layer in terms of its liquefaction potential through appropriate laboratory tests.

A realistic assessment of the integrity of the dam and its ability to remain functional during and after possible seismic events, should consider the complete set of the aforementioned influential parameters with emphasis on the coupling between them.

The computational part of the study must address and evaluate the conditions that exist prior to the anticipated earthquake, the dynamic response of the dam-foundation system and, on the basis of these two steps, the potential for failure. The evaluation process is outlined below,

a. The seepage forces induced by the steady flow of water through the dam and the foundation are evaluated. By utilizing the soil permeability profile for the site, the steady-state pore water pressure field is determined with a finite element seepage analysis. Such evaluation is vital in assessing the effective stress conditions that exist in the embankment and the foundation before any dynamic event occurs. The location of the phreatic surface through the dam section, a critical parameter in the stability aspect, is also determined.

b. The initial effective stress conditions in the dam cross section which represent a key component in the definition of stability is calculated. With elastic soil properties extrapolated from test data for the site and the use of finite element analysis, the steady state stress field is evaluated. The effective soil stress profile that exists prior to a dynamic event is vital in determining the resistance against sliding over potential surfaces and the liquefaction susceptibility of the soil. Effective stresses are the resultant of the soil overburden stresses and the pore water pressure.

c. The dynamic response of the embankment/foundation system is obtained. Since the concern over the integrity of the dam stems basically from its ability to withstand earthquake loads, the way the modeled dam responds to such loads is the most vital step in determining its integrity. The dynamic analysis should be able to provide the stress time histories throughout the structure during an earthquake. In turn, the stress history combined with the steady state stress conditions will become the basis of the safety criteria for both slope stability and liquefaction. A realistic description of the oil conditions and of the appropriate for the site seismic input is needed. From the soil properties definition standpoint, the hysteretic damping is a key parameter in determining the dynamic response. Because of uncertainties surrounding the true level of damping, it is wise to treat this property parametrically. The finite element analysis utilized in the evaluation of the dynamic response is linear in character but it treats the soil as a two-phase medium. While the drawback of linearity is somewhat compensated with the equivalent hysteretic damping, it is the two-dimensional pore water/soil sceleton interaction that provides a realistic description of the behavior of the soil in a dynamic mode. The harmonic analysis inverted with the use of Fast Fourier Transform techniques provides the intergranular stress as well as the pore water pressure fluctuation developed throughout the section during the seismic event.

d. On the basis of the steady state and dynamic solution the slope stability is assessed. The failure potential viewed in the form of a factor of safety against slope failure is evaluated by incorporating the initial and the resulted dynamic stresses. Along various potential surfaces where sliding can occur, the dynamic factors of safety are computed and the critical surfaces identified. This process takes place in conjunction with extrapolated values of cohesion and frictional angle of the soil.

e. The liquefaction potential in the dam is finally evaluated. The driving forces in the liquefaction process is the d amic (cyclic) shear stress that is generated in the soil layers and the associated buildup of pore pressures. While a linear analysis cannot predict the increase, it can provide the level of shearing that the soil experiences during the seismic event. This in turn can thus become the basis for assessing the susceptibility to liquefaction using more empirical relationships.

ANALYSIS OF AN EARTHEN DAM

The various phases of the analysis are carried out with the help of finite element analyses. An example of a discretized dam section is shown in Figure 1. The objective is to evaluate the steady-state pore pressure distribution, the initial effective stress state and the dynamic stresses resulting from an earthquake excitation.

Seepage

The distribution of the pore water pressure in the embankment and the foundation layer prior to an earthquake is evaluated through a steady state seepage analysis. The pore pressure distribution will help define the effective stress distribution throughout the model. enables the evaluation of the effective stress in the soil. The governing equation of **steady unconfined seepage** can be seen in the form,

$$k_x \frac{\vartheta h(x,y)}{\vartheta x^2} + k_y \frac{\vartheta h(x,y)}{\vartheta y^2} = 0 \qquad (1)$$

where, $h(x,y)$ = total head and k_x, k_y = soil permeabilities.

The term *unconfined* refers to the undefined location of the phreatic surface. An iterative process is used to locate such surface. The seepage analysis was performed with the help of the ANSYS general purpose finite element program and the distribution of the total head is graphically shown in Figure 2. The pore pressure is deduced from the total head distribution according to the relation,

$$p_f = h - y \tag{2}$$

where p_f, y are the pore pressure and the vertical elevation respectively.

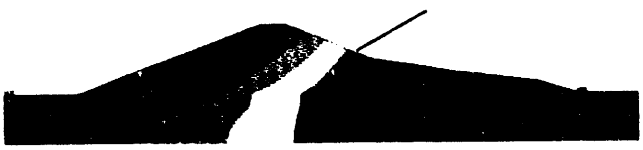

Figure 2. Total Head Profile

Initial Effective Stress State

The stress field prior to a seismic event that exists in the embankment and the foundation layer are an important element in the stability evaluation. The static stress conditions are key components in the definition of the factor of safety against slope failure. Further, the overburden initial stress is vital to a liquefaction potential analysis because of its relation to the effective stress that controls the process of liquefaction. It should also be mentioned that the initial shear stress field has been the focus of a number of investigative works as an influential mechanism in the liquefaction process. It is thus of importance for any analysis to obtain a good description of the initial stress distribution.

The stress field in the system is the result of the soil overburden and of the hydrostatic action of the water in the reservoir. The discretized cross section of the embankment and its foundation are considered to be in a state of plane strain. This computational phase is performed again with the help of the ANSYS program.

The profile of the shear stresses developed from both overburden and steady state seepage is shown in Figure 3. It can be seen that a zone of high stress exists under the downstream face of the dam. The effective overburden stress is finally deduced from the total overburden stress and the steady state pore water pressure.

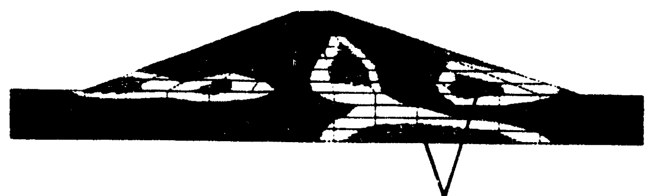

Figure 3. Initial Shear Stress Distribution

Dynamic analysis of the 2-phase medium

In assessing the dynamic effective stress state of the embankment-foundation system, the saturated state of the soil must be accounted for. The pore pressure of the water trapped in the soil skeleton will fluctuate during the earthquake and effect the intergranular soil stresses. Since the strength of the soil is governed by the intergranular stresses, it is important that the dynamic pore pressure be determined. The coupled behavior of pore water and soil skeleton requires that the medium be treated as a two-phase system with governing equations that reflect the coupling.

Further, the ability of the soil to resist liquefaction is dependent on its initial stress state (effective stress) and on the intensity of the dynamic shear stress. The shear stress variation at different locations in the embankment and the foundation as well as the number of stress cycles during the earthquake event determine whether the soil is susceptible to such failure.

Therefore, to effectively analyze the system, the employed model must incorporate;

a. the description of the domain as a two-phase medium.
b. the implementation of actual or representative earthquake input.
c. the evaluation of the time variation of stresses resulting from the seismic input.

In order to perform the dynamic analysis, which satisfies the above requirements, the POROSLAM computer code [3] is employed. The code is a two-dimensional finite element representation of Biot's dynamic equations for both soil and fluid phases. The equations are a description of the response of the soil skeleton and of the pore water in the form,

$$\frac{\vartheta\tau_{xx}}{\vartheta x}+\frac{\vartheta\tau_{xy}}{\vartheta y}=\varrho\ddot{u}_x+\varrho_f\ddot{w}_x$$

$$\frac{\vartheta\tau_{yx}}{\vartheta x}+\frac{\vartheta\tau_{yy}}{\vartheta y}=\varrho\ddot{u}_y+\varrho_f\ddot{w}_y$$

and

$$-\frac{\vartheta p_f}{\vartheta x}=\varrho_f\ddot{u}_x+\frac{1}{f}\varrho_f\ddot{w}_x+\frac{\eta}{k}\dot{w}_x$$

$$-\frac{\vartheta p_f}{\vartheta y}=\varrho_f\ddot{u}_y+\frac{1}{f}\varrho_f\ddot{w}_y+\frac{\eta}{k}\dot{w}_y \qquad (3)$$

where,

$[u_x,u_y]$ = components of displacement of the soil

$[w_x,w_y]$ = components of displacement of the pore water

$$\{\tau\}=(\tau_{xx},\tau_{yy},\tau_{xy})^T=$$

$$\left\{\sigma_{xx}-\alpha p_f,\sigma_{yy}-\alpha p_f,\sigma_{xy}\right\}^T$$

while, f = porosity, ϱ = total mass density, ϱ_f = fluid mass density, α = compressibility of solid, M = compressibilityof the fluid, η = fluid viscosity, and k = soil permeability.

For linear elastic material behavior of the soil skeleton, the resultant equation that relate the total stress vector to the displacement vector including the effect of hysteretic damping, take the form

$$\{\tau\}=E_c\left([D_0]\,[D_1]+[D_3]\,[D_1]\,\frac{\vartheta}{\vartheta t}\right)\{u_x,u_y\}^T+$$

$$\alpha^2M\,[D_2]\,\{u_x,u_y\}^T+\alpha M\,[D_2]\,\{w_x,w_y\}^T \quad (4)$$

where,

$$[D_0]=\begin{bmatrix}1&\frac{\nu}{1-\nu}&0\\\frac{\nu}{1-\nu}&1&0\\0&0&\frac{1-2\nu}{2(1-\nu)}\end{bmatrix}$$

$$[D_3]=\begin{bmatrix}\lambda_c&\frac{\lambda_c\nu}{1-\nu}&0\\\frac{\lambda_c\nu}{1-\nu}&\lambda_c&0\\0&0&\frac{\lambda_s(1-2\nu)}{2(1-\nu)}\end{bmatrix}$$

$$[D_1]=\begin{bmatrix}\frac{\vartheta}{\vartheta x}&0\\0&\frac{\vartheta}{\vartheta y}\\\frac{\vartheta}{\vartheta y}&\frac{\vartheta}{\vartheta x}\end{bmatrix}\qquad[D_2]=\begin{bmatrix}\frac{\vartheta}{\vartheta x}&\frac{\vartheta}{\vartheta y}\\\frac{\vartheta}{\vartheta x}&\frac{\vartheta}{\vartheta y}\\0&0\end{bmatrix}$$

$$p_f=-\alpha M\,(e_{xx}+e_{yy})-M\left(\frac{\vartheta w_x}{\vartheta x}+\frac{\vartheta w_y}{\vartheta y}\right)$$

λ_c is the hysteretic damping ratio associated with hydrostatic compression while λ_s represents the damping ratio associated with shear strains and $E_c=\frac{(1-\nu)E}{(1+\nu)(1-2\nu)}$.

For the linear problem, the solution of the discretized equations is obtained in the frequency domain. The dynamic input, which represents the ground acceleration time history for a particular seismic event, is expressed in terms of its Fourier components and is applied as a forcing function to the base model. The response of the dam cross section to actual earthquakes is evaluated through the Harmonic Unit Response solution of the model.

The implementation of transmiting boundaries, shown in Figure 4, on the two sides of the model allowed for the propagation of waves outward. These boundaries ensure the continuation of both intergranular stresses and pore pressures into the saturated soil. The propagation is based on the one-dimensional wave equations for plane waves through saturated soils.

The ground motions used to excite the model were generated from a power spectrum that is compatible to the Rg. 1.60 response spectrum. The Harmonic Unit Response solution can also be used to provide the response of the dam to earthquakes of different peak accelerations that belong to the same earthquake family. Accordingly, the safety of the dam can be addressed on the basis of the intensity of the ground motion.

FAILURE POTENTIAL OF DAM

The seismic loads that are selected to excite the dam cross section are a combination of vertically propagating shear and P waves. While vertically propagating shear waves are typically used to study the response of a homogeneous horizontal layer, the presense of the embankment constructed over such layer requires the incorporation of vertical plane P waves. These P waves are from the same earthquake family with peak acceleration equal to two thirds (2/3) of the corresponding shear wave and are at different phase.

Slope Stability

The stability of the dam is viewed in terms of a safety factor along any potential failure surface as shown in Figure 4. The margin of safety against sliding can typically be seen as the ratio of the shear strength at a given effective stress to the corresponding shear strength on the envelope line. For this two dimensional analysis, the safety factor is defined in terms of the state of stress at any instant during the seismic event by employing the stress invariants of the intergranular stresses that develop within each element.

Since failure is expected to occur over an entire surface, the safety factor along any such potential surface is defined as a contribution from all the points transversed by the surface as follows,

$$SF = \frac{\sum_i A_i SF_i}{\sum_i A_i} \tag{5}$$

where A_i = area of the finite element transversed by failure surface and $(SF)_i$ = safety factor for element i. The safety factor for an individual element is formed on the basis of the intergranular stress invariants J_1 and J_2' and for materials satisfying the Mohr-Coulomb failure envelope, the safety factor within elements is defined by

$$-\alpha J_1 + \sqrt{J_2'} = k$$

$$J_1 = \sigma_x + \sigma_y + \sigma_z$$

$$J_2' = \frac{\left[(\sigma_x - \sigma_y)^2 + (\sigma_y - \sigma_z)^2 + (\sigma_z - \sigma_x)^2\right]}{6} + \tau_{xy}^2 \tag{6}$$

$$k = \frac{3C}{\sqrt{9 + 12tan^2\phi}} \qquad \alpha = \frac{tan\phi}{\sqrt{9 + 12tan^2\phi}}$$

such that

$$SF_i = \frac{k + \alpha J_1}{\sqrt{J_2'}} \tag{7}$$

The parameters C and ϕ are the usual cohesion and friction angle used in soil mechanics.

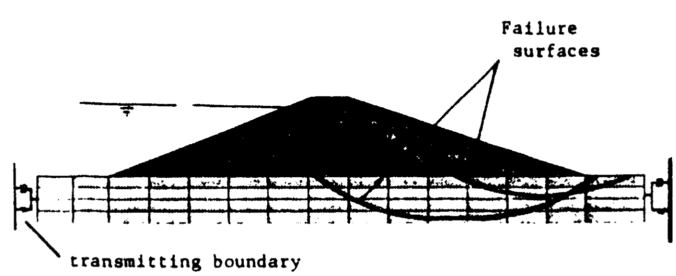

Figure 4. Potential Failure Surfaces

Because of the assumed linearity of the constitutive equations, the computed dynamic stresses that will result from a scaled-up earthquake will be subject to similar increase, except for the effects of the hysteresis. The amplification of the fluctuation of the intergranular stresses and pore pressures will, at various times of the seismic duration, bring the stress state of the points closer to the failure envelope causing significant reduction of the safety factor. This issue is addressed with the evaluation of the safety factor over a chosen failure surface subject to incremental changes of the peak acceleration of the same earthquake. Figure 5 depicts the effect of the seismic intensity on the factor of safety.

The role of the frictional angle on the slope stability is also examined. The effect on the factor of safety is profound and it stems from the fact that ϕ defines the failure envelope. Figure 6 shows the comparison between the analysis using the POROSLAM code and a quasi-static analysis code. It is apparent that the finite element dynamic analysis calculates higher safety factors against slope sliding.

The assumed level of hysteretic damping has a considerable effect on the induced dynamic stresses. Figure 7 shows the peak shear stresses that result from a vertically propagating shear wave at different elevations of the embankment's centerline.

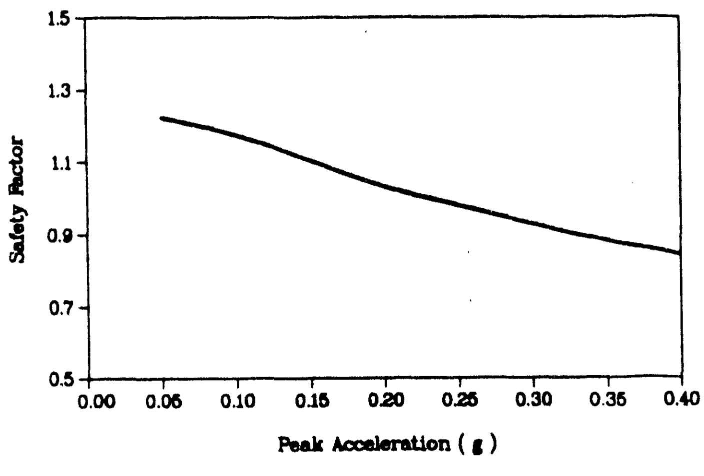

Figure 5. Effect of Earthquake Intensity on Safety Factor

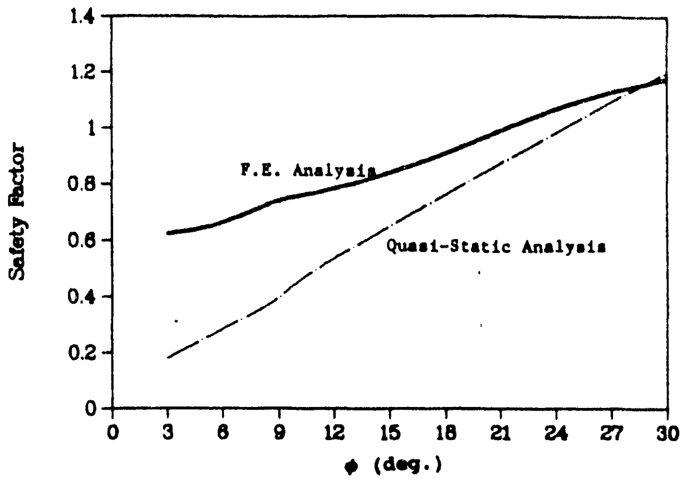

Figure 6. Effect of Frictional Angle on Safety Factor

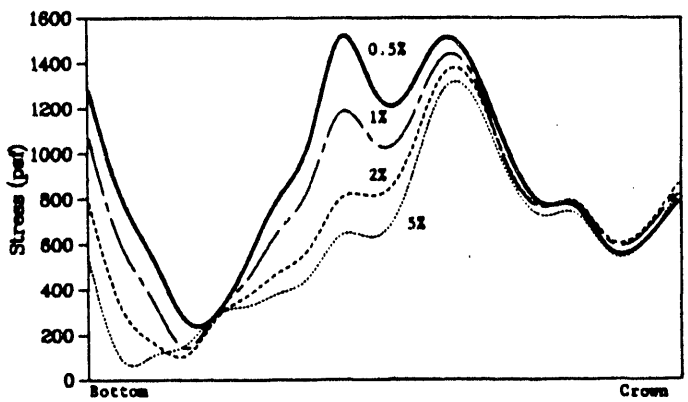

Figure 7. Effect of Damping on Dynamic Shear Stresses

Liquefaction Potential

Liquefaction is considered the phenomenon associated with the loss of strength of a cohesionless soil during an earthquake. The mechanism is identified as one permitting the movement of soil in a large deformation scenario. On the basis of our knowledge that is deduced from laboratory tests and field observations, the matrix of influential parameters includes the characteristics of the soil type (sand, silt, clay etc.), its relative density, the initial confining stress (effective stress) and the earthquake input (in terms of both the intensity and the duration).

Despite the linear character of the response analysis, important conclusions can still be drawn regarding the likelihood of liquefaction failure. It should be emphasized that the behavior of the soil during liquefaction is highly nonlinear. What a linear analysis can achieve is the following: with available laboratory test data on threshold values of strain or stresses, beyond which liquefaction failure is induced, a comparison can be made between these test data and calculated strains or stresses states from the linear analysis. Given that for small soil deformations and pre-liquefaction conditions a linear analysis is applicable, locations of potential failure can be identified. Further, estimates of the safety margins can be deduced indicating how far from the triggering of liquefaction is the soil in these critical zones. The assessment of the liquefaction potential is deduced with the implementation of the following conventional procedure;

a. The earthquake likely to occur in the vicinity of the site is determined and is applied as base motion (base in this case is the stiff rock below the weak layer).

b. The time history of the intergranular shear stresses or $\sqrt{J_2'}$ due to the propagation of waves are deduced from the response of the embankment and the foundation layer. The intensity of the induced stresses and their time variation are evaluated and the critical zones are identified.

c. To enable comparisons with laboratory tests, which are subject on uniform cyclic loading, the calculated stress time histories are idealized into equivalent uniform stress cycles.

d. The critical stresses that can cause liquefaction when applied as uniform cycles must be determined. This soil property may be viewed either as shear strength or as critical values of $k + \alpha J_1$ and it can be obtained from representative samples of soil from the site reflecting the relative density, the confining pressure and the penetration resistance. This strength value at the particular location is compared against the induced shear or stress invariant $\sqrt{J_2'}$.

To predict liquefaction in homogeneous soil layers a number of tests have been conducted using cyclic triaxial compression loading. Results are available in terms of the stress ratio

$\frac{\sigma_{dc}}{2\sigma_a}$ that induces liquefaction in **10** and **30** cycles (σ_{dc} is the cyclic deviatoric stress and σ_a is the initial ambient pressure that the soil sample was consolidated under). The stress ratio $\frac{\tau}{\sigma_0}$ that causes liquefaction under field conditions is corrected to the laboratory value. In the field, the stress ratio links the shear stress that developes at a location (converted to uniform cycles) and the initial effective stress σ_0 (associated with the overburden and pore pressure). Because it is observed that the threshold shear is proportional to the relative density D_r, extrapolation of the test data to different soils is possible.

It should be emphasized that in the case of a dam, results pertaining to the failure due to primarily shear in homogeneous layers should be used with extreme caution. Alternatively, the critical stress invariant $\sqrt{J_2'}$ can be estimated from similar laboratory tests and compared with the one resulting from the evaluation. This will lead to more realistic assessment of the liquefaction susceptibility in the embankment of the dam. The potential to failure due to shear can still be used in the lower portion of the foundation layer where shear conditions will still dominate.

The criterion that defines the potential to liquefaction can be viewed in the form,

$$LQF = \frac{Shear \quad strength \quad \tau\,(N_{equiv} \quad cycles)}{Max. \quad cyclic \quad shear \quad (0.65\tau_{max})}$$

for the shear mode, or equivalently

$$LQF = \frac{\sqrt{J_2'}_{soil \quad testing}}{\sqrt{J_2'}_{seismically \quad induced}} \tag{8}$$

for complex stress state, where LQF = liquefaction potential ($LQF > 1.0$: no liquefaction).

Figure 8 depicts the variation of $\sqrt{J_2'}$ along the centerline of the dam under the seismic loads described earlier. Given the threshold values of the invariant along the same line (from test data extrapolation) one can identify the critical zones where liquefaction can be triggered.

The effect of different families of earthquakes on the response of the dam cross section is shown in Figure 9. The dynamic shear stresses induced by a 0.2g Charleston-like earthquake are compared with the same stresses induced by a 0.2g earthquake from a Reg. 1.60 spectrum. Both earthquakes are applied as vertically propagating shear waves. Also shown are the stresses resulting from the combination of vertically propagating shear and P waves that derive from the Reg. 1.60 spectrum.

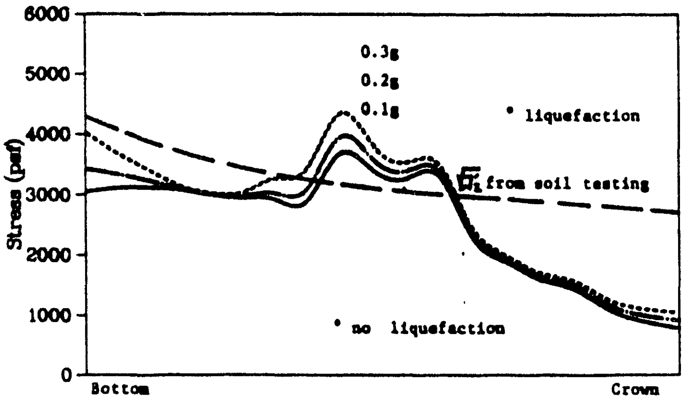

Figure 8. $\sqrt{J_2'}$ Along Centerline of Dam

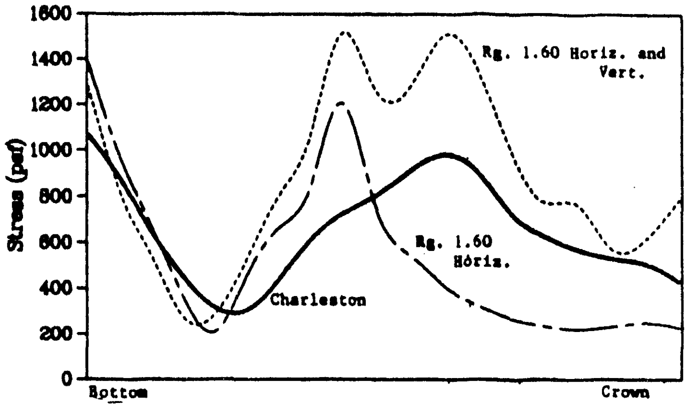

Figure 9. Effect of Various Ground Motions on Shear Stresses

REFERENCES

[1] Y.H. Huang, *Stability Analysis for Slopes. User's Manual on REAME and SWASE computer Programs*, 1988.

[2] ANSYS Engineering Analysis Systems. Swanson Analysis Systems Inc., 1989.

[3] R.H. Lung, *Seismic Analysis of Structures Embedded in Saturated Soils*, Ph.D. Thesis, Department of Civil Engineering, City University of New York, 1980.

[4] N.Simos, C.J. Costantino and C. Miller, *POROSLAM. Two-Dimensional Dynamic Solution of Elastic Saturated Porous Media*, Earthquake Research Center, City University of New York, 1988.

[5] C.J. Costantino, N. Simos, Y.T. Gu, *Seismic Risk Assessment of Small Earthdams*, Technical Report NCEER-91, Earthquake

Research Center, City University of New York, 1991.

[6] W.P. Creager, J. D. Justin and J. Hinds, *Engineering for Dams, Vol I*, 1944.

[7] *Liquefaction of Soils During Earthquakes*, Committee on Earthquake Engineering *et al*, National Academy Press, 1985.

[8] H.B. Seed, I.M. Idriss, *A simplified Procedure for Evaluating Soil Liquefaction Potential*, Report No. EERC 70-9, 1970.

[9] H.B. Seed, I.M. Idriss, *Analysis of Soil Liquefaction: Niigata Earthquake*, Journal of Soil Mechanics and Foundations Division, pp 83-108, 1967.

[10] *Evaluation of Soil Liquefaction Potential for Level Ground During Earthquakes*, NUREG-0026, 1976.

[11] *Representation of Irregular Stress Time Histories by Equivalent Uniform Stress Series in Liquefaction Analyses*, California University, PB-252 635, 1975.

[12] K.L. Lee, H.B. Seed, *Cyclic Stress Conditions Causing Liquefaction of Sands*, Journal of Soil Mechanics and Found. Div., No. SM1, pp.47-70, 1967.

[13] W.D.L. Finn, G.R. Martin, M.K.W. Lee, *Comparison of Dynamic Analyses for Saturated Sands*, Proc. of the ASCE Geotech. Div., Vol.1, pp. 472-491, 1978.

[14] J.M. Ferrito, J.B. Forest, G. Wu, *Compilation of Cyclic Triaxial Liquefaction Test Data*, Geotechnical Testing Journal, Vol 2, No.2, pp. 106-113, 1979.

[15] *The Generation and Dissipation of Pore Water Pressures During Soil Liquefaction*, California University, PB-252 648, 1975.

END

DATE
FILMED
2/10/94